Energy 347 (2026) 140421

Contents lists available at ScienceDirect

Energy

journal homepage: www.elsevier.com/locate/energy

Hierarchical model predictive control of greenhouse energy systems considering energy-water-carbon-food nexus

Dong Lin [a], Minjie Hu [a], Zhiling Ren [a], Yun Dong [a,b,*], Xianming Ye [b], Yuling Fan [c], Lijun Zhang [d]

[a] Faculty of Electrical and Control Engineering, Liaoning Technical University, Huludao 125100, China
[b] Department of Electrical, Electronic and Computer Engineering, University of Pretoria, Pretoria 0002, South Africa
[c] College of Informatics, Huazhong Agricultural University, Wuhan, 430074, China
[d] Department of Electrical and Electronic Engineering, Department of Mechanical and Mechatronic Engineering, Stellenbosch University, Stellenbosch 7600, South Africa

ARTICLE INFO

Keywords:
Greenhouse
Carbon emissions
Renewable energy
EWCF nexus
Model predictive control

ABSTRACT

Greenhouse cultivation plays a vital role in ensuring food security but is often associated with high energy consumption, water usage, and carbon emissions. Integrating renewable energy systems for power supply and utilizing rainwater harvesting for irrigation can help address these challenges. However, balancing these interconnected factors requires advanced control strategies. In this study, we propose a hierarchical model predictive control (MPC) framework to optimize the management of grid-connected photovoltaic-battery systems in greenhouses, accounting for the interactions among energy use, water consumption, carbon emissions, and food production (EWCF nexus). The hierarchical MPC is structured in three layers: the first optimizes greenhouse operations to minimize total costs (MTC); the second manages the scheduling of the hybrid energy system to minimize operational cost (MOC); and the third designs an MPC controller to handle photovoltaic generation and load demand disturbances. Results show that the proposed MTC strategy reduces the total cost by 81.01% compared with the minimizing energy consumption strategy. Moreover, the MOC strategy reduces operational costs by 20.68% compared to the maximizing self-consumption strategy. In addition, the proposed MPC achieves superior performance in tracking the reference trajectory under varying disturbance levels compared to commonly used open loop controllers. This study provides practical guidance for greenhouse management by addressing key resource and environmental challenges, contributing to the sustainable development of controlled-environment agriculture.

1. Introduction

1.1. Challenges of greenhouse cultivation

Greenhouse cultivation is a modern agricultural technique that creates a controlled environment to optimize crop growth by regulating key factors such as temperature, humidity, light intensity, and CO_2 concentration [1]. By providing a stable growing environment, greenhouses protect crops from adverse weather conditions, such as extreme temperatures, heavy rainfall, and strong winds, while also minimizing the impact of pests and diseases [2,3]. In addition, greenhouse systems allow for the extension of the growing season and enable year-round or off-season production. As a result, compared to traditional open-field farming, greenhouse cultivation typically achieves higher yields and better crop quality [4,5]. Although greenhouse cultivation has many advantages, it also faces several challenges, such as high energy consumption, water consumption, and carbon emissions [6,7].

Energy consumption is one of the most significant concerns, as maintaining the controlled environment requires substantial energy inputs. In some greenhouses, energy costs account for more than 70% of the total operating costs due to high energy consumption. The energy consumed is primarily concentrated in heating, ventilation, cooling, supplemental lighting, and irrigation [8]. Heating is typically the largest contributor, accounting for around 70%–80% of total energy use, especially in colder climates [9]. Ventilation, cooling, supplemental lighting, and irrigation each contribute a relatively small proportion to the overall energy consumption. Ventilation and cooling systems consume energy to control temperature and humidity, ensuring optimal conditions for plant growth. Supplemental lighting is used to provide additional light, especially in regions with limited natural sunlight,

* Corresponding author at: Department of Electrical, Electronic and Computer Engineering, University of Pretoria, Pretoria 0002, South Africa.
E-mail address: u24126714@tuks.co.za (Y. Dong).

https://doi.org/10.1016/j.energy.2026.140421
Received 4 May 2025; Received in revised form 24 January 2026; Accepted 10 February 2026
Available online 11 February 2026
0360-5442/© 2026 The Authors. Published by Elsevier Ltd. This is an open access article under the CC BY license (http://creativecommons.org/licenses/by/4.0/).

Nomenclature

A_{pv}	Area of the PV array (m^2)	p_f	Feed-in tariff (R/kWh)
C_b	Battery rated capacity (kWh)	P_E	Artificial lighting power (W/m^2)
c_n	Unit capacity cost of battery (Rand/kWh)	P_{pv}	Power output from PV array (kW)
C_{air}	CO_2 concentration (g/m^3)	C_{oper}	Operating costs (R)
C_{assi}	CO_2 assimilation (g/m^2 s)	Q_c	Heating/cooling power (W/m^2)
C_{cap}	Greenhouse heat capacity (J/m^2 °C)	Q_{cov}	Heat transfer across cover (W/m^2)
C_{carb}	Cost of supplemental CO_2 (R)	Q_{lamp}	Lamp heating power (W/m^2)
C_{elec}	Electricity cost (R)	Q_{rad}	Solar radiation power (W/m^2)
C_{inj}	CO_2 injection (g/m^2 s)	Q_{sun}	Incoming radiation power (W/m^2)
C_{out}	Outside CO_2 concentration (g/m^3)	Q_{trans}	Transpiration power (W/m^2)
$C_{p,air}$	Air heat capacity (J/kg °C)	Q_{vent}	Heat loss through ventilation power (W/m^2)
C_{vent}	Ventilation's influence on CO_2 levels (g/m^2 s)	r_b	Resistance parameter (s/m)
e_a	Average vapor pressure	r_s	Stomatal resistance (s/m)
e_s	Saturation vapor pressure	RH_{air}	Greenhouse relative humidity (%)
ET	Crop evapotranspiration (ton/s)	R_n	Net radiation at crop level
g_c	The condensation conductance (m/s)	s_r	Shading rate
g_e	Transpiration conductance (m/s)	S	The greenhouse area (m^2)
g_v	Ventilation speed (m/s)	SOC	State of charge (%)
h	Height of greenhouse (m)	T_{air}	Greenhouse temperature (°C)
H_{air}	Greenhouse humidity (g/m^3)	T_{cell}	PV cell temperature (°C)
H_{air}^{sat}	Saturated vapor concentration (g/m^3)	T_{ref}	Reference temperature (°C)
I_{con}	Water consumed for irrigation (ton)	T_{out}	Outdoor temperature (°C)
k	Temperature coefficient (°C)	α_1	Transmission coefficient
k_c	Crop factor	α_2	Heat transfer coefficient (W/m^2 °C)
k_1	Maximum change rates of Q_c	β_{cal}	Calendar aging
k_2	Maximum change rates of g_v	β_{cyc}	Cycle aging
k_3	Maximum change rates of C_{inj}	δ	Vapor pressure curve slope
k_4	Maximum change rates of s_r	ϵ	Latent-to-sensible heat ratio
L	Energy required for evaporation (J/g)	η	Lighting heat conversion factor
LAI	Leaf area index	η_c	Coefficient of charging efficiency
L_{cyc}	Life cycle number of the battery	η_d	Coefficient of discharging efficiency
p_c	Supplied CO_2 price (R/ton)	η_{pv}	Efficiency of PV power generation
p_{gc}	Parameter linked to condensation surface properties (m/s $°C^{1/3}$)	γ	Crop specific parameter
		λ_p	Pumping volume to power conversion coefficient
p_p	Peak electricity price (R/kWh)	λ_v	Ventilation rate to power conversion coefficient
p_s	Standard electricity price (R/kWh)	μ	Psychometric constant
p_o	Off-peak electricity price (R/kWh)	ρ_{air}	Density of air, (kg/m^3)
p_e	Electricity price (R/kWh)		

supporting photosynthesis [10]. The irrigation system consumes energy mainly for the operation of water pumps.

Water consumption in greenhouse operations is also a critical issue. Greenhouses can reduce irrigation water use by 50%–90% compared to open-field cultivation [11]. However, the need for irrigation remains significant, especially in larger-scale operations. Despite employing the highly water-efficient irrigation system, greenhouse cultivation still demands around 1.5 l of water per square meter per day [12]. In addition, cooling systems, particularly evaporative cooling, rely heavily on water, adding to the overall consumption.

In addition to the high consumption of energy and water resources, greenhouse operations are often associated with a considerable carbon footprint [13]. For many modern greenhouses, especially those requiring active climate control, more than 60% of their energy consumption comes from fossil fuels, leading to considerable carbon emissions [14]. This not only accelerates climate change, but also poses risks to local ecosystems and biodiversity.

The challenges of greenhouse operations are particularly severe in South Africa, where frequent electricity shortages occur as the national grid often fails to meet electricity demand. To manage these shortages and prevent grid collapse, the country regularly implements load shedding (planned rolling blackouts). For example, users experienced more than 1030 h of power outages in just the first half of 2023 [15]. In addition, South Africa's heavy reliance on coal-fired power generation (as shown in Fig. 1) has contributed to a grid emission factor of 708 g CO_2/kWh in 2023, which is among the highest in the world and has helped make it the 14th largest greenhouse gas emitter globally. Moreover, water scarcity poses another significant concern, with prolonged droughts affecting several regions [16]. For instance, Cape Town narrowly avoided "Day Zero" in 2018, when municipal water supplies were nearly depleted.

1.2. Overview of existing research

To address the energy challenges in greenhouse cultivation, several methods have been proposed to improve energy efficiency and promote sustainability. In [18,19], energy-efficient heating and cooling systems have been developed, along with advanced lighting systems designed to minimize power usage while maintaining optimal light levels for plant growth. In [20,21], the integration of renewable energy sources, such as solar and wind power, into greenhouse operations has been explored to reduce dependence on conventional energy supplies and enhance environmental sustainability. In [22], the feasibility of creating net-zero energy greenhouses through the integration of semitransparent organic solar cells into greenhouse structures is examined. The findings indicate that organic solar cells can offset greenhouse energy demands in warm and moderate climates while maintaining sufficient sunlight for plant needs. In addition, the integration of rooftop greenhouses with

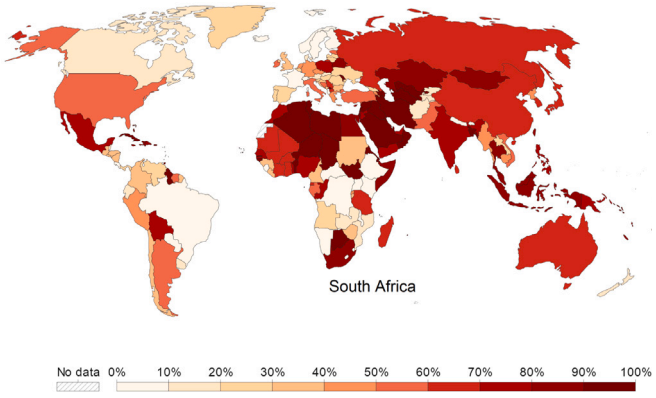

Fig. 1. Share of electricity production from fossil fuels [17].

buildings has been developed to optimize greenhouse operations and reduce energy consumption and operational costs [23].

Various methods have been proposed to deal with water consumption issues in greenhouse operations. In [24], a drip irrigation system was introduced to deliver water directly to plant roots, minimizing evaporation and runoff, which improved water use efficiency and crop yields. In [25], a humidification-dehumidification system integrated with a solar still is used to reduce water consumption in greenhouses. This system harnesses solar energy to produce 4.03–5.20 m^3/day of water through condensation, recycling moisture from the air and reusing it for irrigation, thereby significantly reducing the dependence on external freshwater sources.

To address the challenges of greenhouse carbon emissions, several energy-efficient technologies have been explored. In [26], a comprehensive optimization method for the shading and electrical performance of a roof-mounted photovoltaic system in a Venlo-type greenhouse is proposed, achieving an annual carbon emission reduction of 11,202 kg. In [27], geothermal energy was examined as a sustainable option for heating and cooling greenhouses, utilizing stable underground temperatures as an eco-friendly alternative to fossil fuels. In [28], biomass combined heat and power systems were implemented, generating both heat and electricity from renewable biomass resources, further lowering the environmental impact. In [29], a combined cooling heating and power system is optimized using deep learning algorithms to capture CO_2 emissions from micro power plants for greenhouse enrichment, resulting in a 56% reduction in CO_2 emissions.

Although research on greenhouse energy, water, and carbon emissions has led to important advancements in energy efficiency, water conservation, and carbon emissions reduction, several challenges still persist. First, many studies on greenhouse operation optimization focus on only one of the key factors such as energy consumption, water usage, carbon emissions, or crop yield, while few consider these factors simultaneously. These factors are interrelated and can significantly influence each other [30]. For example, optimizing for minimal energy consumption might lead to reduced ventilation and cooling, which in turn can increase water usage due to higher humidity levels [31]. Similarly, a focus on maximizing crop yield often requires increased energy and water consumption, which can elevate carbon emissions. The energy-water-carbon-food (EWCF) nexus is illustrated in Fig. 2. Addressing only one factor may compromise the balance of other essential factors, affecting the overall sustainability of greenhouse operations [32].

Second, although numerous studies have proposed optimization methods for greenhouse energy systems, most focus on individual components, such as HVAC performance or energy storage operation, without fully considering the integration of PV systems with the electrical grid [33]. The combination of PV systems, energy storage, and grid connection can significantly enhance the flexibility and reliability of greenhouse energy management.

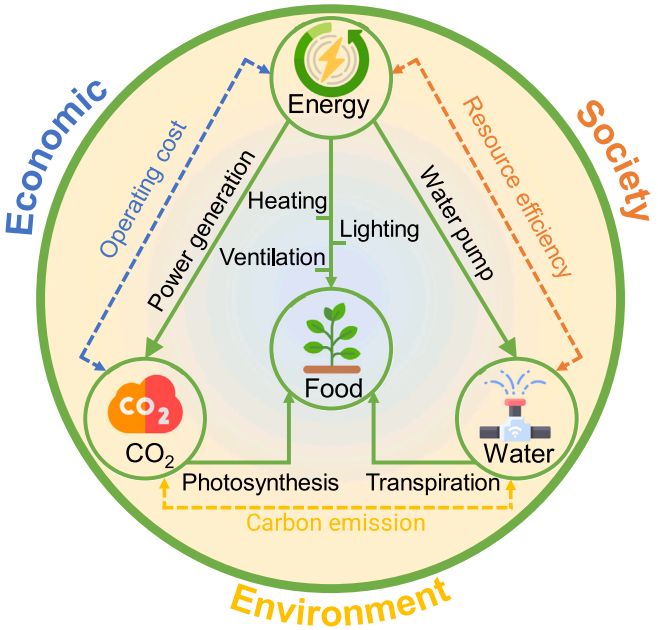

Fig. 2. EWCF nexus of greenhouse systems.

Third, few studies have focused on control strategies for greenhouse hybrid energy systems under the uncertainties associated with PV power generation and load demand. These uncertainties, caused by factors such as weather variability and changing energy consumption patterns, significantly affect system stability and efficiency. Methods such as stochastic optimization and model predictive control (MPC) offer promising solutions to manage these uncertainties and improve system performance under variable conditions [34].

1.3. Research contributions

To address the challenges of greenhouse cultivation, this study introduces a hybrid energy system that integrates PVs, batteries, and the grid to supply power to the greenhouse. A hierarchical model predictive control approach is proposed to manage this system, considering the EWCF nexus. The framework consists of three layers: a greenhouse operation optimization layer, an energy system management layer, and a real-time controller layer. The system is analyzed under South African conditions, providing a comprehensive evaluation of its performance and applicability in addressing regional environmental and resource challenges. The main contributions of this research are:

(1) We propose a grid-connected greenhouse hybrid energy system that combines PV generation, battery storage and the utility grid to replace the traditional grid-only supply, aiming to alleviate power shortages and reduce greenhouse gas emissions in regions with frequent outages and carbon-intensive electricity.
(2) We develop a three-layer hierarchical model predictive control framework that coordinates greenhouse operation optimization, hybrid energy system scheduling and real-time power-flow control, while explicitly accounting for the EWCF nexus.
(3) We formulate a total cost minimization strategy for greenhouse operation that integrates electricity cost, CO_2 supply cost and CO_2 emission cost, enabling operation that simultaneously reduces energy use, emissions and operating cost while maintaining suitable growing conditions.
(4) We design an MPC-based hybrid energy management strategy that accounts for battery aging and carbon-emission costs to enhance real-time power-flow control under PV and load uncertainties.

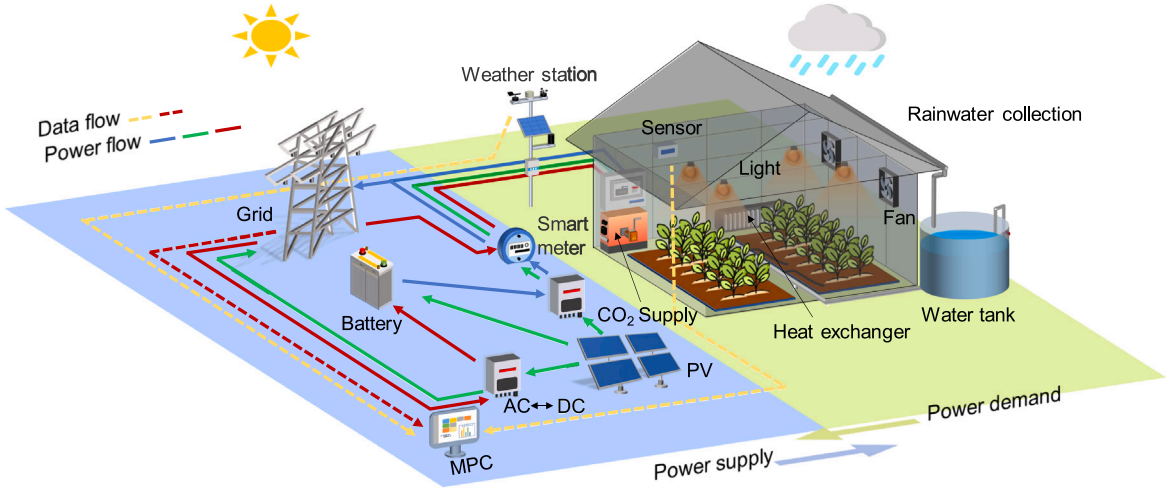

Fig. 3. Greenhouse hybrid energy system.

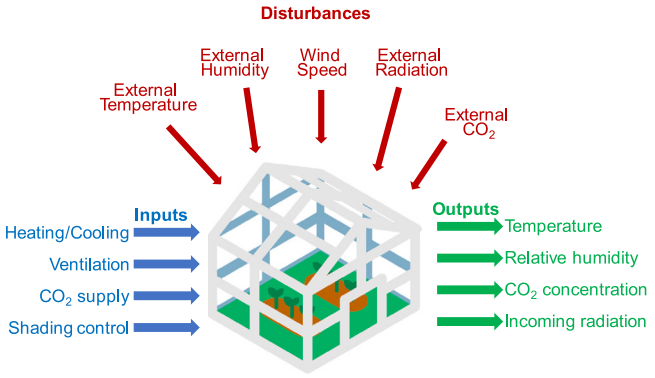

Fig. 4. Schematic diagram of a greenhouse system.

The rest of the paper is structured as follows. Section 2 describes the model of the greenhouse hybrid energy system. Section 3 presents the hierarchical MPC strategy. Section 4 analyzes the simulation results to evaluate the effectiveness of the proposed control strategy. Section 5 concludes the paper by summarizing key points and highlighting directions for future research.

2. System description

Fig. 3 illustrates the hybrid energy system proposed in this study, which integrates PV generation, battery storage, and grid power to supply a smart greenhouse. The system is coordinated by a smart meter and an MPC controller to ensure efficient energy distribution in response to varying power demands.

2.1. Greenhouse system

Fig. 4 shows a schematic diagram of a greenhouse system. In this study, the greenhouse model described in [35,36] is used.

2.1.1. Temperature

Regulating the temperature is essential for optimizing plant growth, preventing disease, and maintaining a suitable environment [37]. The temperature model is expressed as:

$$\frac{dT_{air}}{dt} = \frac{1}{C_{cap}}(Q_{sun} + Q_{lamp} - Q_{cov} - Q_{trans} - Q_{vent} + Q_c), \tag{1}$$

where T_{air} denotes the internal temperature, C_{cap} refers to the greenhouse heat capacity, Q_{sun} is the incoming radiation power, Q_{lamp} accounts for the heat generated by the lamps, Q_{cov} represents the heat loss through the cover, Q_{trans} is the energy absorbed by crop transpiration, Q_{vent} signifies the energy loss due to ventilation, and Q_c represents the heating/cooling power.

$$Q_{sun} = \alpha_1(1 - s_r)Q_{rad}, \tag{2}$$

where α_1 is the cover's transmission coefficient, s_r represents the shading rate, and Q_{rad} is the power of solar radiation.

Q_{cov} can be expressed as:

$$Q_{cov} = \alpha_2(T_{air} - T_{out}), \tag{3}$$

where α_2 represents the cover heat transfer coefficient, T_{out} represents the outdoor temperature.

Q_{trans} can be acquired through:

$$Q_{trans} = g_e L(H_{crop} - H_{air}), \tag{4}$$

where g_e denotes transpiration conductance, L signifies the energy utilized for water evaporation from a leaf, H_{crop} indicates the absolute water vapor concentration at the crop level, H_{air} represents the absolute water vapor concentration. g_e is acquired through:

$$g_e = \frac{2LAI}{(1+\epsilon)r_b + r_s}, \tag{5}$$

where LAI is the leaf area index, ϵ is the ratio of latent to sensible heat content of saturated air, r_b is the boundary layer resistance, and r_s is the stomatal resistance.

H_{crop} is given by:

$$H_{crop} = H_{air,sat} + \epsilon\frac{r_b}{2LAI}\frac{R_n}{L}, \tag{6}$$

where $H_{air,sat}$ denotes the saturated vapor concentration. $H_{air,sat}$ can be expressed by:

$$H_{air,sat} = 5.5638e^{0.0572T_{air}}. \tag{7}$$

ϵ and r_s can be acquired through:

$$\epsilon = 0.7584e^{0.0518T_{air}}. \tag{8}$$

$$r_s = (82 + 570e^{-\gamma\frac{R_n}{LAI}})(1 + 0.023(T_{air} - 20)^2), \tag{9}$$

where γ stands for a crop parameter, R_n signifies the net radiation at the crop level.

$$R_n = 0.86(1 - e^{-0.7LAI})(Q_{sun} + P_E), \tag{10}$$

where P_E is the electrical power consumption of the lamps.

$$Q_{lamp} = \eta P_E. \tag{11}$$

$$Q_{vent} = g_v \rho_{air} C_{p,air} (T_{air} - T_{out}), \tag{12}$$

where g_v is the rate of ventilation, ρ_{air} denotes the air density, $C_{p,air}$ represents the air heat capacity.

2.1.2. Relative humidity

Precise humidity control is key to a stable and productive cultivation environment. Maintaining proper relative humidity in a greenhouse is essential for plant health and climate control. Optimal humidity supports efficient water absorption and prevents stress while reducing risks of fungal diseases and mold. Excess humidity can hinder nutrient uptake and photosynthesis, impacting growth [38]. The relative humidity RH_{air} is determined as follows:

$$RH_{air} = H_{air} / H_{air,sat}, \tag{13}$$

where H_{air} represents the air vapor concentration and is obtained by:

$$\frac{dH_{air}}{dt} = \frac{1}{h}(H_{trans} - H_{cov} - H_{vent}), \tag{14}$$

where H_{trans} is the water vapor generated by transpiration, H_{cov} represents the water vapor condensation on the cover and H_{vent} signifies the water vapor movement due to ventilation, h denotes the height of the greenhouse.

H_{trans} can be characterized by:

$$H_{trans} = g_e(H_{crop} - H_{air}). \tag{15}$$

H_{cov} can be acquired through:

$$H_{cov} = g_c \left[0.2522 e^{0.0485 T_{air}} (T_{air} - T_{out}) - (H_{air,sat} - H_{air}) \right], \tag{16}$$

$$g_c = \begin{cases} 0 & \text{if} \quad T_{air} \le T_{out} \\ p_{gc}(T_{air} - T_{cov})^{1/3} & \text{if} \quad T_{air} > T_{out}. \end{cases} \tag{17}$$

H_{vent} can be gained via:

$$H_{vent} = g_v(H_{air} - H_{out}), \tag{18}$$

where g_v represents the ventilation rate.

2.1.3. Carbon dioxide concentration

Controlling CO_2 concentration is vital in greenhouses to enhance plant growth and maximize photosynthesis efficiency. The model is given by:

$$\frac{dC_{air}}{dt} = \frac{1}{h}(C_{inj} - C_{assi} - C_{vent}), \tag{19}$$

where C_{air} represents the CO_2 concentration within the greenhouse, C_{inj} denotes the rate of CO_2 injection, C_{assi} signifies the CO_2 assimilation, and C_{vent} stands for the changes in CO_2 concentration due to ventilation.

C_{assi} and C_{vent} can be calculated by:

$$C_{assi} = 2.2 \times 10^{-3} \frac{1}{1 + \frac{0.42}{C_{air}}} (1 - e^{-0.003(Q_{sun} + P_E)}), \tag{20}$$

$$C_{vent} = g_v(C_{air} - C_{out}). \tag{21}$$

2.1.4. Light intensity

Adequate light promotes optimal plant development, enhances flowering, and boosts yield. Insufficient light can slow growth, weaken plants, and reduce productivity, while excessive light can lead to overheating and stress. By controlling light intensity within ideal ranges, greenhouse growers can ensure consistent, healthy crop growth, supporting both quality and quantity in crop production [39]. Light intensity can be determined using Eq. (2) and is not repeated here.

2.1.5. Greenhouse irrigation

Precision irrigation provides plants with the exact amount of water needed, optimizing growth while conserving resources [40]. The crop water requirement is estimated through evapotranspiration ET. The irrigation model is given by [41]:

$$\frac{dI_{con}}{dt} = ET. \tag{22}$$

$$ET = k_c \times \frac{0.408 \Delta R_n + \mu \frac{1713}{T_{air}+273}(e_s - e_a)}{\Delta + 1.64\mu}, \tag{23}$$

where k_c is the crop coefficient, Δ stands for the slope of the vapor pressure curve, μ is the psychometric constant, e_s signifies the saturation vapor pressure, e_a denotes the average vapor pressure.

$$\Delta = \frac{4098 \times e_s}{(T_{air} + 237.3)^2}, \tag{24}$$

$$e_a = e_s \times RH_{air}, \tag{25}$$

$$e_s = 0.6108 \times \exp\left(\frac{17.27 \times T_{air}}{T_{air} + 237.3}\right). \tag{26}$$

Efficient water management is essential for greenhouse operations, especially in regions facing water scarcity or variable rainfall [42]. Traditionally reliant on municipal water or groundwater, greenhouses are under increasing pressure to adopt sustainable practices that reduce environmental impact and conserve resources. A viable solution is combining rainwater harvesting and groundwater extraction for irrigation. Rainwater collected from the greenhouse roof is stored and used as the primary water source, reducing dependence on municipal supplies and lowering costs. In times of insufficient rainfall, groundwater serves as a backup, ensuring a reliable water supply. This dual approach optimizes water use, provides resilience against drought, and supports healthier plant growth, as rainwater is free from harmful chemicals. By integrating both methods, greenhouses can conserve freshwater resources and minimize their ecological footprint.

2.2. Hybrid energy system

A hybrid energy system, comprising PVs, batteries, and the power grid, enables flexible energy management and enhances supply stability. PV generation efficiently harnesses solar energy during the day to provide clean power, but its intermittent nature limits continuous supply. Batteries supplement power during low PV output or peak demand periods, balancing supply and demand and extending renewable energy usage. The power grid serves as a backup source, ensuring reliability, especially when PV generation is unstable or battery capacity is insufficient [43]. Through optimized configuration and coordinated control, this system achieves higher self-consumption, reduces energy costs, and lowers carbon emissions, advancing sustainable energy utilization.

Fig. 5 illustrates the hybrid energy system. P_1 represents the power discharged from the battery to supply the greenhouse, P_2 is the power used by the PV system to charge the battery, P_3 corresponds to the power generated by the PV system for the greenhouse, P_4 refers to the power fed into the grid, P_5 represents the power supplied by the grid to the greenhouse, and P_6 is the power drawn from the grid to charge the battery. The model of the hybrid energy system is displayed below.

2.2.1. PV panels

Based on [44], PV power generation can be determined by:

$$P_{pv} = Q_{rad} A_{pv} \eta_{pv} \left[1 + k \times (T_{cell} - T_{ref})\right], \tag{27}$$

where P_{pv} is the hourly power output of the PV system, η_{pv} indicates the efficiency of the PV array, A_{pv} refers to the area of the PV panels, k is the temperature coefficient, T_{ref} represents the reference temperature of the PV cells, T_{cell} is the actual temperature of the PV cells, which can be determined as follows:

$$T_{cell} = T_{air} + 0.0256 \times Q_{rad}. \tag{28}$$

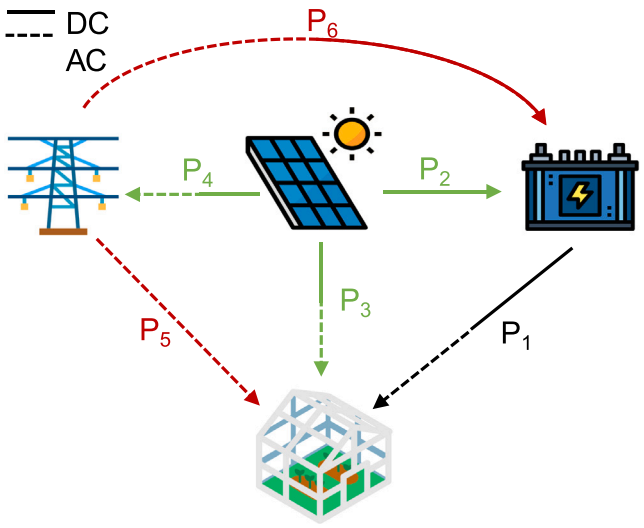

Fig. 5. Power flow of hybrid energy systems.

2.2.2. Battery bank

The SOC of the battery is determined by:

$$SOC(k) = SOC(0) + \frac{\eta_c}{C_b}\sum_{i=1}^{k}\left[P_2(i) + P_6(i)\right] - \frac{1}{\eta_d C_b}\sum_{i=1}^{k} P_1(i), \tag{29}$$

where $SOC(k)$ is the SOC of the battery at the kth hour, $SOC(0)$ is the initial SOC, η_c is the charging efficiency, η_d is the discharging efficiency, C_b is the battery capacity.

2.2.3. Electric grid

This study adopts a time-of-use (TOU) tariff, with electricity prices defined as follows [45]:

$$p_e = \begin{cases} p_o & t \in [23,24] \cup [0,7] \\ p_s & t \in [7,10] \cup [15,18] \cup [21,23] \\ p_p & t \in [10,15] \cup [18,21] \end{cases}, \tag{30}$$

where p_o, p_s, and p_p are the electricity prices during the off-peak, standard, and peak periods, respectively. In addition, the feed-in tariff p_f is equal to p_o.

2.3. Model performance and applicability

The greenhouse model used in this study is based on the work of [35,36], which developed and validated a Venlo-type greenhouse model in the Netherlands. This model demonstrated high accuracy, with a strong correlation coefficient (r) and low root mean square error (RMSE) between measured and simulated values, confirming its effectiveness in predicting energy consumption and environmental conditions. Its reliability has supported its adoption in numerous studies aimed at optimizing energy use and environmental control. Similarly, the hybrid energy system models, including PV panels, energy storage, and grid interaction, are based on validated models. These models are well-established in energy research, showing robustness in simulating energy production, storage dynamics, and grid interactions under diverse conditions, making them suitable for greenhouse energy systems.

Given this study's focus on optimizing and controlling the greenhouse hybrid energy system rather than developing or experimentally validating individual component models, further experimental validation was not conducted. Although validation for South African conditions was not specifically performed, the climatic similarities between South Africa and the Netherlands, particularly in terms of solar radiation, seasonal temperature fluctuations, and humidity patterns, support the applicability of these models to South African greenhouse systems.

3. Hierarchical model predictive control

This study proposes a hierarchical MPC method, as illustrated in Fig. 6. The hierarchical structure consists of three layers: the greenhouse operation optimization layer, the hybrid energy system management layer, and the real-time control layer. The first layer determines the optimal energy demand based on greenhouse operations, which is used by the second layer to schedule energy resources accordingly, while the third layer tracks the scheduled actions in real time to ensure accurate system execution.

3.1. First layer: greenhouse system operation optimization

In previous studies, greenhouse operation optimization has mostly focused on strategies such as minimizing energy consumption (MEC) or minimizing energy costs (MCE), often overlooking the impact of carbon emissions during the operation process. This study converts the environmental impact of carbon dioxide into carbon emission costs and proposes a total cost minimization (MTC) method that considers both greenhouse operational costs and carbon emission costs to enhance the overall operational performance of the greenhouse.

3.1.1. Optimization objective function

The objective function for the proposed MTC strategy is defined as follows:

$$J_{tot} = C_{oper} + C_{emis}, \tag{31}$$

where C_{oper} is the operating cost, C_{emis} is the carbon emissions cost.

C_{oper} can be calculated by:

$$C_{oper} = C_{elec} + C_{carb} \tag{32}$$

where C_{elec} is the electricity cost, C_{carb} is the CO_2 supply cost.

C_{elec} can be determined using:

$$C_{elec} = C_h + C_v + C_i, \tag{33}$$

where C_h represents the cost of heating and cooling the greenhouse, C_v denotes the ventilation cost, C_i stands for the irrigation cost.

$$C_h = \int_{t_i}^{t_f} Q_c(t) p_e(t) S dt, \tag{34}$$

$$C_v = \int_{t_i}^{t_f} g_v(t) p_e(t) \frac{Q_f S}{V_f} dt, \tag{35}$$

where Q_f represents the ventilation fan's rated power, and V_f is the airflow volume per hour at the rated power.

Although irrigation costs encompass various factors, including the construction and maintenance of rainwater harvesting systems, groundwater extraction equipment, water treatment, and potential environmental impacts, this research focuses on the energy consumption of irrigation pumps. By concentrating on this aspect, the study aims to provide a precise assessment of energy-related expenses that can be directly optimized, aligning with the primary objective of enhancing greenhouse energy management. The cost is determined by the irrigation water demand and electricity price, assuming the electricity rate during irrigation remains consistently at the off-peak level. C_i can be calculated by:

$$C_i = p_o Q_p \frac{I_{con}}{V_p}, \tag{36}$$

$$I_{con} = \int_{t_i}^{t_f} ET(t) dt, \tag{37}$$

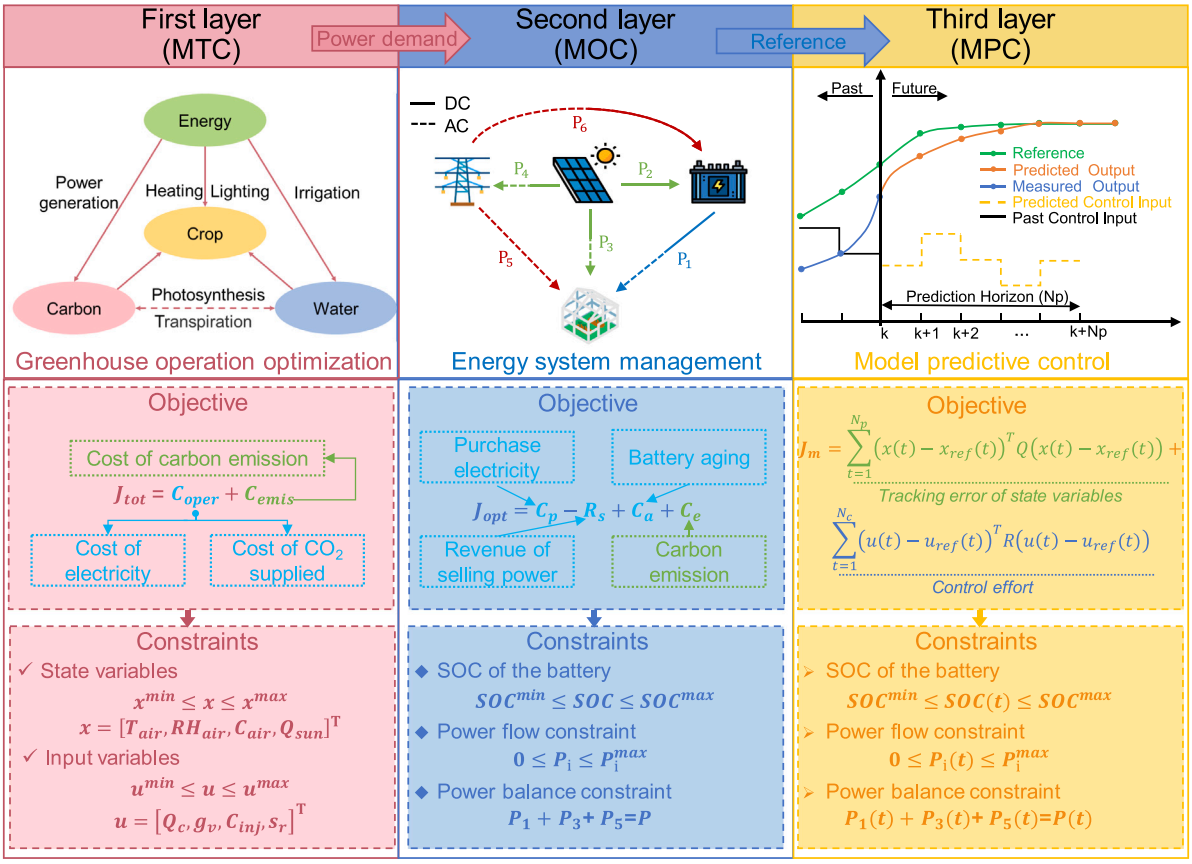

Fig. 6. Hierarchical model predictive control structure.

where Q_p is the rated power of the pump, V_p is the volume of water pumped, I_{con} is the volume of water consumed.

C_{carb} can be obtained by:

$$C_{carb} = \int_{t_i}^{t_f} p_c C_{inj}(t) S dt, \tag{38}$$

where p_c represents the CO_2 price.

The CO_2 emissions can be calculated by:

$$C_{emis} = C_{equi} - C_{abso}, \tag{39}$$

$$C_{equi} = k_{eq} E_{elec}, \tag{40}$$

$$E_{elec} = \int_{t_i}^{t_f} (Q_c(t)S + Q_v(t)S + \frac{Q_p ET(t)}{V_p}) dt, \tag{41}$$

$$C_{abso} = \int_{t_i}^{t_f} C_{assi}(t) S dt, \tag{42}$$

where C_{equi} denotes the CO_2-eq emissions, calculated using the consumed electrical energy E_{elec} and the grid emission factor k_{eq}.

3.1.2. Greenhouse system constraints

In greenhouse cultivation, maintaining environmental factors (state variables) within optimal ranges is essential to prevent yield reduction [46]. For instance, excessively high temperatures can lead to crop wilting or death, while insufficient CO_2 levels hinder photosynthesis. Growers can define these constraints based on personal experience or determine them through optimization techniques aimed at maximizing crop yield or profit. State constraints can be described as:

$$T_{air}^{min} \le T_{air} \le T_{air}^{max}, \tag{43}$$

$$RH_{air}^{min} \le RH_{air} \le RH_{air}^{max}, \tag{44}$$

$$C_{air}^{min} \le C_{air} \le C_{air}^{max}, \tag{45}$$

where T_{air}^{min}, RH_{air}^{min}, and C_{air}^{min} represent the minimum acceptable values for temperature, relative humidity, and CO_2 concentration, respectively. T_{air}^{max}, RH_{air}^{max}, and C_{air}^{max} represent their upper limits.

The shading rate constraints can be defined as:

$$\begin{cases} s_r = 0, & \text{if } Q_{sun} \le Q_{sun}^{min} \\ 0 < s_r \le 1, Q_{sun}^{min} \le Q_{sun}(1 - s_r), & \text{if } Q_{sun} > Q_{sun}^{min} \end{cases} \tag{46}$$

The input constraints can be described as:

$$Q_c^{min} \le Q_c \le Q_c^{max}, \tag{47}$$

$$g_v^{min} \le g_v \le g_v^{max}, \tag{48}$$

$$C_{inj}^{min} \le C_{inj} \le C_{inj}^{max}, \tag{49}$$

$$s_r^{min} \le s_r \le s_r^{max}, \tag{50}$$

where Q_c^{min}, g_v^{min}, C_{inj}^{min}, and s_r^{min} are the minimum values for heating/cooling power, ventilation rate, CO_2 supply rate and shading rate, respectively. Q_c^{max}, g_v^{max}, C_{inj}^{max}, and s_r^{max} set the corresponding upper limits.

To reduce actuator wear from frequent adjustments, the following constraints on the rate of change are implemented:

$$\left| \frac{Q_c}{dt} \right| \le k_1, \tag{51}$$

$$\left|\frac{g_v}{dt}\right| \le k_2, \tag{52}$$

$$\left|\frac{C_{inj}}{dt}\right| \le k_3, \tag{53}$$

$$\left|\frac{s_r}{dt}\right| \le k_4, \tag{54}$$

where k_1, k_2, k_3, and k_4 represent the maximum rates of change for Q_c, g_v, C_{inj}, and s_r, respectively.

The MTC strategy is formulated as minimizing the objective function (31) with the constraints (45)–(54).

3.2. Second layer: hybrid energy system management

The second layer effectively manages the operational cost optimization of the hybrid energy system by considering the dynamic interactions of energy flows and state of charge (SOC) within the system. By generating reference trajectories for SOC and power flow, it ensures that the system remains economically viable while adhering to operational constraints. This foundational management of energy resources prepares the system for further optimization in the next layer, which focuses on real-time tracking and control to ensure precise implementation of the strategies developed in the second layer.

3.2.1. Objective function

In this study, a strategy for minimizing the operational cost (MOC) is proposed, and the objective function J_{opt} is represented by:

$$J_{opt} = C_p - R_s + C_a + C_e, \tag{55}$$

where C_p is the cost of purchasing electricity, R_s is the revenue from selling electricity, C_a is the cost associated with battery aging, C_e is the carbon emissions cost.

$$C_p = (P_5 + P_6)p_e, \tag{56}$$

$$R_s = P_4 p_f. \tag{57}$$

$$C_a = (\beta_{cal} + \beta_{cyc})c_n B_c, \tag{58}$$

where β_{cal} is the calendar aging cost, β_{cyc} signifies the cost related to cycle aging, c_n represents the per-unit cost of battery capacity, encompassing both initial investment and upkeep expenses, B_c is the battery rated capacity.

β_{cal} can be calculated by [47]:

$$\beta_{cal}(t) = 6.6148 \times 10^{-6} \times SOC(t) + 4.6404 \times 10^{-6}. \tag{59}$$

β_{cyc} can be obtained by:

$$\beta_{cyc}(t) = \int_{t_i}^{t_f} \frac{\frac{1}{\eta_d}P_1(t) + \eta_c(P_2(t) + P_6(t))}{2C_b L_{cyc}} dt, \tag{60}$$

where L_{cyc} is the life cycle number of the battery.

$$C_e = C_{eq} SCC, \tag{61}$$

$$C_{eq} = \int_{t_i}^{t_f} e_f(P_5(t) + P_6(t))dt, \tag{62}$$

where C_{eq} represents the amount of CO_2-*equivalent* emissions, while e_f stands for the grid's carbon emission factor, which reflects the carbon emissions per unit of electricity generated.

3.2.2. Hybrid energy system constraints

The system constraints include the boundaries for SOC, a terminal condition for SOC, constraints on power flow, and the requirement for power balance. The SOC boundary is defined as:

$$SOC^{min} \le SOC \le SOC^{max}, \tag{63}$$

where SOC^{min} is the lower limit of SOC of the battery, and SOC^{max} is the upper limit of SOC.

The SOC terminal state constraint is expressed as:

$$SOC(24) \ge SOC(0). \tag{64}$$

The power flow constraint is given by:

$$0 \le P_i \le P_i^{max}, (i = 1, 2, \dots, 6), \tag{65}$$

where P_i^{max} is the upper limit of P_i.

The power balance constraint is expressed as:

$$P_2 + P_3 + P_4 = P_{pv}, \tag{66}$$

where P_{pv} is the power generated by PVs.

The power demand of greenhouse loads P, which is obtained from the upper layer optimization, needs to be met.

$$P_1 + P_3 + P_5 = P. \tag{67}$$

Charging and discharging operations are mutually exclusive and cannot occur simultaneously.

$$P_1 P_2 = 0. \tag{68}$$

$$P_1 P_6 = 0. \tag{69}$$

The proposed optimization approach for hybrid energy system operation aims to minimize the objective function (55), while adhering to constraints (63)–(69).

In this study, the proposed hybrid energy system management strategy is compared with a commonly used rule-based strategy for maximizing self-consumption of clean energy (MSC). The MSC strategy optimizes hybrid energy systems by prioritizing the use of local renewable energy and battery storage, minimizing grid reliance, and maximizing energy efficiency [48]. The pseudo-code for the MSC algorithm is presented in Algorithm 1.

Algorithm 1 MSC Algorithm

```
Input: PV generation, load, battery SOC
if PV generation ≥ load then
    Use PV generation to supply load
    Charge battery with excess PV generation
    if battery full then
        Sell excess PV generation to the grid
    end if
else
    Use PV generation
    Discharge battery to meet deficit
    if battery insufficient then
        Use grid power
    end if
end if
Output: Optimal power flow: PV generation to load, battery charge/discharge, sold to the grid
```

3.3. Third layer: MPC controller design

MPC is a powerful tool for optimizing the operation of hybrid energy systems [49]. MPC can handle the dynamic nature of energy systems by predicting future disturbances and adjusting energy flows in real-time [50]. By optimizing the use of PV energy, battery storage, and

grid power, MPC can ensure that the greenhouse has a reliable energy supply while minimizing operational costs and environmental impacts.

This layer employs real-time MPC to track reference trajectories generated by the second layer, minimizing deviations in both state and input variables in real-time to ensure optimal system performance. MPC is crucial for managing greenhouse hybrid energy systems due to their complexity, dynamic nature, and exposure to disturbances. MPC optimizes energy usage by predicting future states, efficiently using renewable energy, reducing operational costs, and minimizing carbon emissions. Its capability to manage multiple objectives, such as balancing energy supply and demand, extending battery life, and responding to both environmental changes and unexpected disturbances, makes MPC a powerful and adaptive tool. The layered structure of MPC further enhances control precision and coordination across different system components.

In this study, the continuous-time state-space model of the battery is given by:

$$\dot{x}(t) = f\big(x(t), u(t)\big), \tag{70}$$

where the state and input vectors are defined as

$$x(t) = \mathrm{SOC}(t),$$
$$u(t) = \begin{bmatrix} P_1(t) \\ P_2(t) \\ P_3(t) \\ P_4(t) \\ P_5(t) \\ P_6(t) \end{bmatrix}. \tag{71}$$

Based on the battery energy balance, the continuous-time state equation can be written as

$$f\big(x(t), u(t)\big) = \frac{1}{C_b}\left(\eta_c\big(P_2(t) + P_6(t)\big) - \frac{1}{\eta_d}P_1(t)\right), \tag{72}$$

where C_b is the battery capacity, and η_c and η_d are the charging and discharging efficiencies, respectively. To facilitate the controller implementation, (72) is discretized with sampling interval T_s as

$$x(k+1) = f_d\big(x(k), u(k)\big), \tag{73}$$

where k is the current sampling instant kT_s, and

$$f_d\big(x(k), u(k)\big) = x(k) + T_s\, f\big(x(k), u(k)\big). \tag{74}$$

Based on the discrete-time state-space model (73), the MPC objective function is defined as

$$\begin{aligned} J_m = &\sum_{k=1}^{N_p}\big(x(k) - x_{\mathrm{ref}}(k)\big)^{\mathrm{T}} Q\big(x(k) - x_{\mathrm{ref}}(k)\big) \\ &+ \sum_{k=1}^{N_c}\big(u(k) - u_{\mathrm{ref}}(k)\big)^{\mathrm{T}} R\big(u(k) - u_{\mathrm{ref}}(k)\big), \end{aligned} \tag{75}$$

where $x(k)$ and $u(k)$ denote the predicted state and input at the kth step within the prediction and control horizons, respectively.

The MPC strategy can be formulated as solving the optimization problem defined by the objective function (75), subject to the discrete-time dynamics (73)–(74) and to the admissible control state space characterized by constraints (63)–(69). At each time step, the optimization problem is solved over a prediction horizon; however, only the first control input from the optimized sequence is applied to the system. The process is then repeated at the next time step with updated system states and predictions in a receding horizon fashion. This approach ensures that the controller continuously adjusts to real-time system conditions, providing robustness and adaptability. The pseudocode for the MPC algorithm is shown in Algorithm 2.

Algorithm 2 MPC algorithm

1: **Initialize** system state $x(0)$
2: **for** each time step t **do**
3: Measure the current system state $x(t)$
4: Solve the optimization problem to minimize the objective function (75)
5: Subject to system dynamics and constraints (63) to (69)
6: Apply the first control input $u^*(t)$
7: Discard the remaining control inputs
8: Update the system state: $x(t+1)$
9: **end for**

Table 1
Greenhouse system parameters.

Parameter	Value	Unit	Parameter	Value	Unit
A_{pv}	5000	m^2	p_p	3.1047	R/kWh
C_{cap}	30 000	J/m^2 °C	r_b	150	s/m
$C_{p,air}$	1003	J/kg °C	S	40 709	m^2
C_b	1500	kWh	α_1	0.7	–
c_n	3000	R/kWh	α_2	10	W/°C m^2
h	7	m	γ	0.008	–
k	-3.7×10^{-3}	$°C^{-1}$	ρ_{air}	1.225	kg/m^3
L	2450	J/g	λ_v	0.3	kW/m^3
LAI	2.6	–	λ_p	0.06	W/m^3
L_{cyc}	10 000	–	η	75	%
p_{gc}	1.8×10^{-3}	m/s $°C^{1/3}$	η_c	95	%
p_o	0.5157	R/kWh	η_d	95	%
p_s	0.9446	R/kWh	η_{pv}	15	%
SCC	900	R			

4. Simulation

4.1. Simulation data

In this study, a Venlo-type greenhouse with a total area of 40,709 m^2 and an average height of 7 m is investigated. The greenhouse is outfitted with 4536 SON-T lamps to provide necessary artificial lighting. To maintain optimal temperatures, air-to-water heat exchangers with a coefficient of performance of 3.5 for both heating and cooling are installed every 80 m^3. Ventilation is provided by axial plate fans, each with a power output of 300 W and an airflow rate of 5000 m^3/h. The greenhouse utilizes an OCAP (Organic CO_2 for Assimilation by Plants) network to supply CO_2 at a cost of R 1000 per ton. The parameters for the greenhouse system are derived from [35] and are presented in Table 1, while the system constraints are outlined in Table 2. Meteorological data, obtained from a weather station located at the University of Pretoria (−25.75308037°S, 28.22859001°E). Specifically, weather data from August 8, 2023, is selected to represent a typical winter day in the region, characterized by lower ambient temperatures and moderate solar radiation. The weather profile is illustrated in Fig. 7. The optimization problems are solved using the 'fmincon' solver with the sequential quadratic programming algorithm in MATLAB. The detailed optimization results are provided below.

4.2. Optimization of the greenhouse system

4.2.1. Results of MTC strategy

The results of the MTC strategy are shown in Fig. 8. Subplots (a) to (d) represent the optimized results of the control variables. Subplots (e) to (h) show the optimized results of environmental factors: temperature, relative humidity, CO_2 concentration, and light intensity, respectively. The green, yellow, and red background colors represent off-peak, standard, and peak electricity price periods, respectively.

In subplot (a), it can be observed that the greenhouse only undergoes heating without cooling. This is because the outside temperature is relatively low, requiring additional heat to offset the losses due to

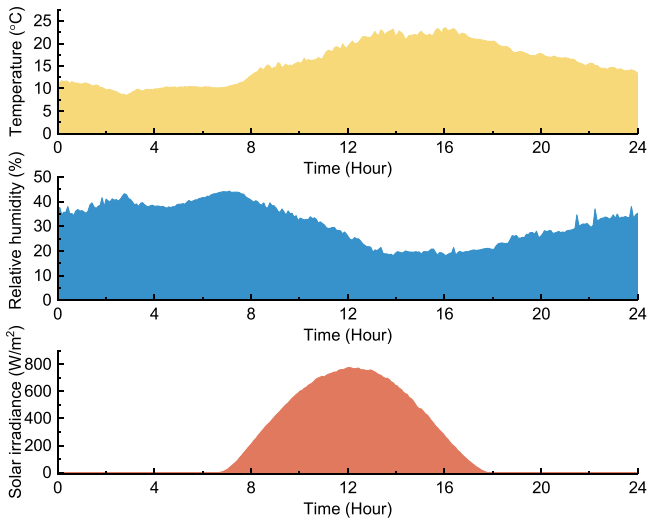

Fig. 7. Weather data for August 8, 2023.

Table 2
System constraints.

Variable	Value	Unit	Variable	Value	Unit
C_{air}^{max}	2000	ppm	RH_{air}^{max}	90	%
C_{air}^{min}	400	ppm	SOC^{max}	95	%
C_{inj}^{max}	0.02	g/m^2 s	SOC^{min}	10	%
C_{inj}^{min}	0	g/m^2 s	T_{air}^{max}	26	°C
g_v^{max}	0.02	m/s	T_{air}^{min}	14	°C
g_v^{min}	0	m/s	P_1^{max}	700	kW
k_1	0.17	W/m^2 s	P_2^{max}	1000	kW
k_2	1.67×10^{-5}	m/s^2	P_3^{max}	1000	kW
k_3	1.67×10^{-5}	g/m^2 s	P_4^{max}	1000	kW
k_4	3.33×10^{-4}	s^{-1}	P_5^{max}	800	kW
Q_c^{max}	200	W/m^2	P_6^{max}	500	kW
Q_c^{min}	−200	W/m^2			

heat exchange with the external environment, thereby maintaining the greenhouse temperature within the desired range. Subplot (e) shows that the internal temperature of the greenhouse is lowest in the morning, close to the lower limit (14 °C). As heating progresses, and with the increase in external temperature and solar radiation, the greenhouse temperature gradually rises, reaching the upper limit (26 °C) around noon, after which the heating power gradually drops to zero.

Subplot (b) reveals that ventilation mainly occurs during midday and the afternoon, as the external temperature is higher during these periods, and ventilation does not lead to significant heat loss. The air exchange with the outside environment reduces the relative humidity, as shown in subplot (f), with the lowest relative humidity levels occurring around noon.

From subplot (c), we see that CO_2 injection occurs mainly between 8:00 and 17:00, a period with strong sunlight, during which photosynthesis is most active and the crop's CO_2 absorption rate is higher compared to other times of the day. To reduce costs, CO_2 levels are maintained at the lower limit (400 ppm), as observed in subplot (g).

Subplot (d) shows that shading primarily occurs around midday when solar radiation exceeds the lower limit (300 W/m^2). Following shading, the solar radiation power is maintained at the lower limit required for crop growth, as illustrated in subplot (h).

4.2.2. Comparison of three optimization strategies

Fig. 9 shows the comparison results between the proposed MTC strategy in this study and the commonly used MEC and MCE strategies

Table 3
Greenhouse electricity demand.

Time	Load (kW)	Time	Load (kW)
0:00–1:00	38.66	12:00–13:00	89.03
1:00–2:00	9.19	13:00–14:00	121.41
2:00–3:00	7.64	14:00–15:00	109.41
3:00–4:00	6.62	15:00–16:00	124.45
4:00–5:00	7.31	16:00–17:00	96.85
5:00–6:00	38.57	17:00–18:00	6.71
6:00–7:00	421.93	18:00–19:00	9.24
7:00–8:00	5.60	19:00–20:00	11.73
8:00–9:00	25.02	20:00–21:00	11.33
9:00–10:00	35.39	21:00–22:00	11.95
10:00–11:00	42.77	22:00–23:00	12.26
11:00–12:00	62.42	23:00–24:00	11.87

in previous research. From subplot (a), it can be observed that the MEC strategy has the lowest energy consumption (1290.27 kWh), followed by the MTC strategy (1317.35 kWh), with the MCE strategy having the highest energy consumption (1542.50 kWh). However, the energy consumption for both the MEC and MTC strategies is mainly concentrated during periods with higher electricity prices, such as peak and standard periods, while the energy consumption during the lower-cost off-peak period is relatively low. As a result, although the MEC and MTC strategies have lower total energy consumption, their energy costs are higher than those of the MCE strategy.

As shown in subplot (b), the energy cost for the MCE strategy is R1986.44, which is lower compared to the MEC strategy (R2218.57) and the MTC strategy (R2199.70), with a reduction of approximately 10.47% and 9.61%, respectively. This illustrates that the load shifting employed in the MCE strategy effectively reduces energy costs despite the higher energy consumption.

From subplot (c), we can find that the total cost of the MTC strategy (R4320.82) is significantly lower compared to the MEC strategy (R22743.70) and the MCE strategy (R23105.46), with reductions of 81.01% and 81.31%, respectively. The reason for this drastic reduction is that the MTC strategy takes a comprehensive approach by considering not only energy costs but also CO_2 supply costs and carbon emission costs. By integrating all these factors, the MTC strategy outperforms both the MEC and MCE strategies in terms of overall economic efficiency. Therefore, compared with conventional MEC and MCE strategies that do not explicitly take the EWCF nexus into account, using the proposed MTC strategy can substantially reduce the overall greenhouse operational cost while maintaining comparable energy consumption.

4.3. Optimization of the hybrid energy system

In this study, the electricity demand shown in Table 3, calculated using the MTC strategy, is adopted as the reference for energy supply. This approach ensures that the energy supply aligns with the demand projections optimized for cost efficiency, providing a structured framework for managing energy resources effectively.

4.3.1. Results of the MOC strategy

Fig. 10 shows the results of the MOC strategy. The power flows from the PV system, battery, and grid are dynamically adjusted throughout the day. In the early morning, the system relies on battery power (P_1) and grid power (P_5) to meet greenhouse demand, while during the midday, solar power (P_3) is predominantly used to supply the greenhouse, with excess energy either charging the battery (P_2) or being fed back into the grid (P_4). At night, the battery charges from the grid (P_6) during low price periods, preparing for use during peak demand. This strategy ensures the system optimizes energy usage, reduces reliance on high-cost grid electricity, and maximizes cost savings.

Fig. 11 shows the battery SOC optimization results. During the early morning (00:00–07:00), the battery discharges to the greenhouse

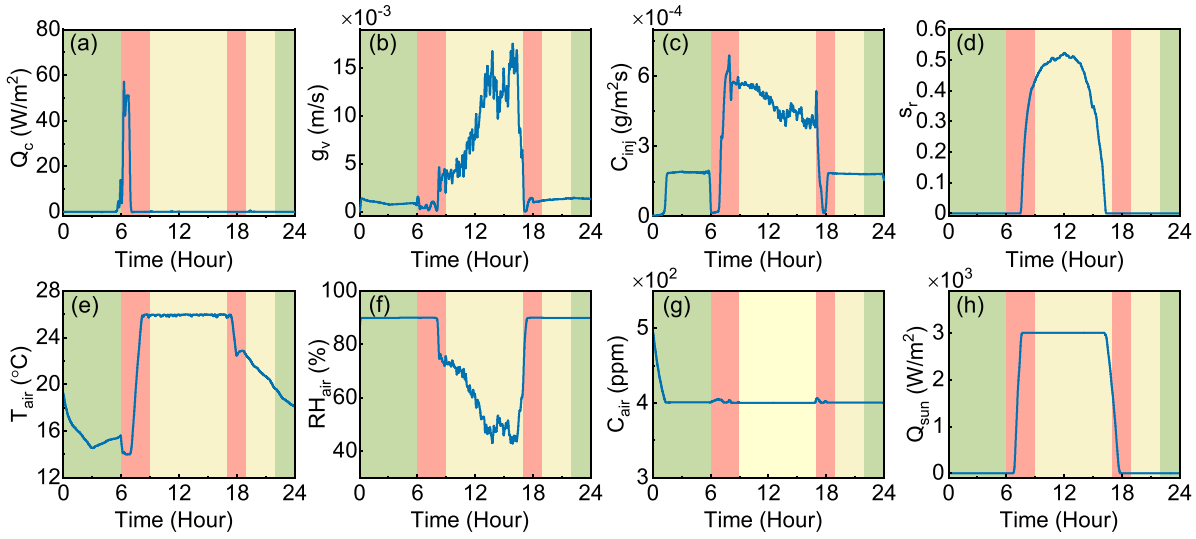

Fig. 8. Results of MTC strategy.

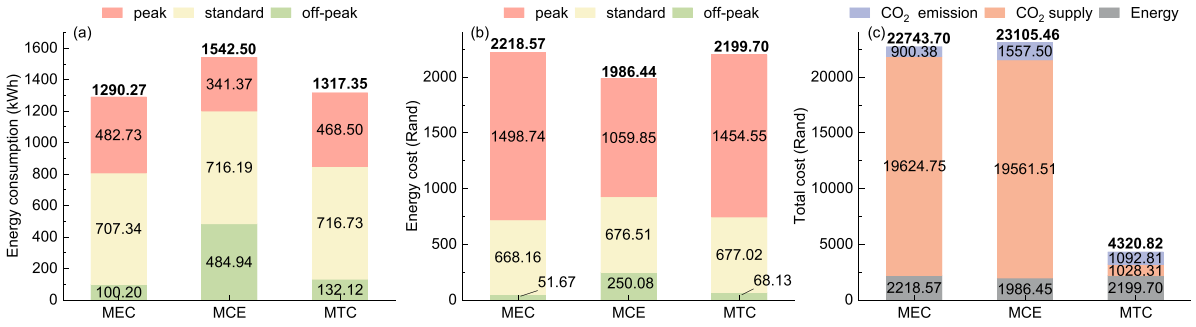

Fig. 9. Comparison of three greenhouse operation optimization strategies.

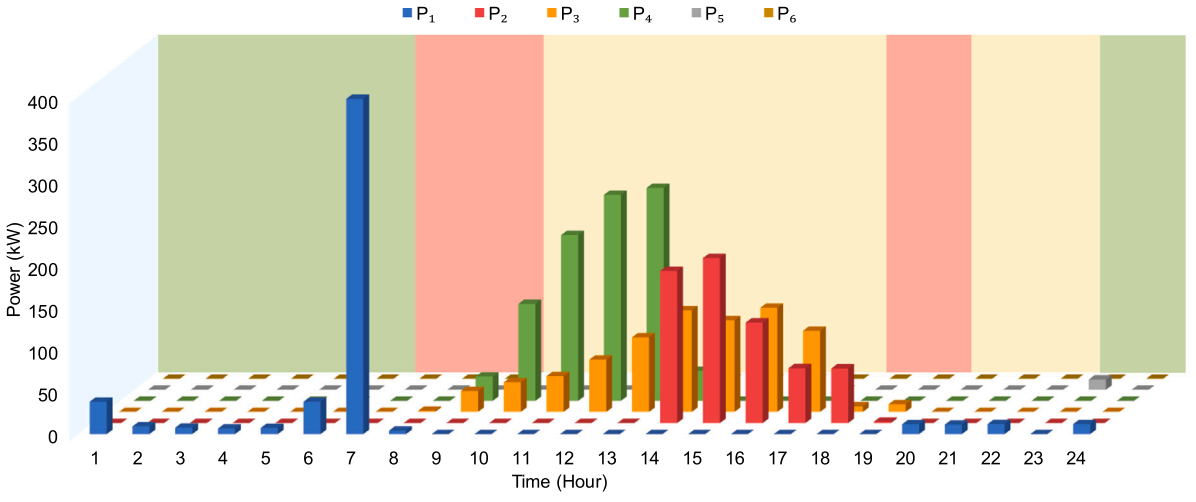

Fig. 10. Operation optimization results of hybrid energy systems.

($-P_1$), causing the SOC to drop from around 60% to approximately 30%. This discharge reduces reliance on grid electricity during peak hours, minimizing costs. In the afternoon period (14:00–18:00), the battery recharges from the PV system (P_2), gradually restoring the SOC to about 60%. This strategy optimizes battery usage by prioritizing discharging during peak periods (6:00–7:00) and charging when solar or grid electricity is most economical, effectively reducing the total operational costs while maintaining a balanced SOC.

Fig. 12 shows the power flow distribution for P_1, P_3, and P_5 across different pricing periods. For P_1, the majority of power consumption

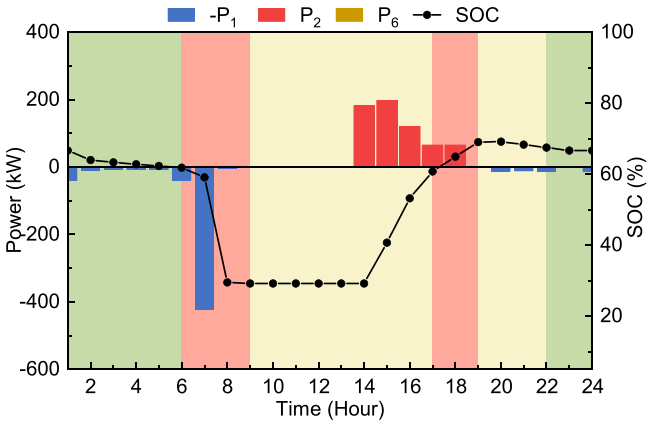

Fig. 11. Battery SOC optimization results.

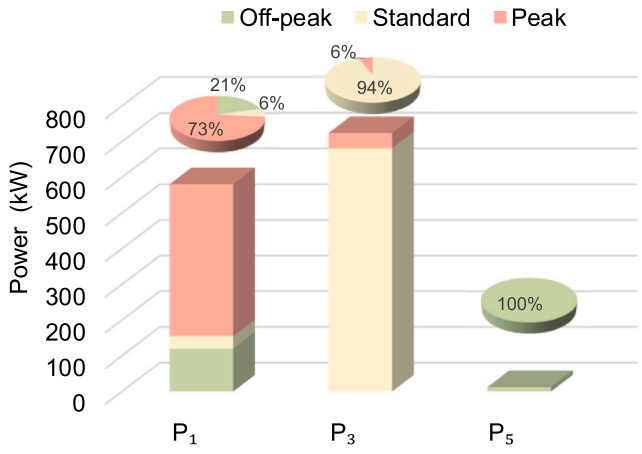

Fig. 12. Power flow distribution during different periods.

occurs during the peak period (73%), with smaller proportions during the standard (6%) and off-peak (21%) periods, indicating a higher cost associated with energy usage. For P_3, the PV supply to the greenhouse, occurs mainly in the standard period (94%), with minimal use during peak. For P_5, all energy consumption occurs during the off-peak period, showing a cost-effective strategy that maximizes savings by avoiding peak and standard periods.

Fig. 13 illustrates the real-time energy allocation under different operating conditions. To make the analysis clearer, three typical scenarios are defined based on the time-of-use electricity price, PV availability, and the greenhouse load profile over a typical day. Scenario 1 (06:00–08:00) represents the morning peak-load and peak-price period, during which most of the greenhouse demand is supplied by the battery P_1, significantly reducing grid consumption. Scenario 2 (08:00–19:00) corresponds to the daytime high-irradiance period, where PV power P_3 becomes the dominant source and the surplus PV is used to charge the battery P_2 or is sold back to the grid P_4 (see Fig. 10). Scenario 3 (19:00–24:00 and 0:00–06:00) covers the off-peak night period without solar generation, in which the grid P_6 is mainly used to recharge the battery at low prices, while the small residual load is directly supplied by the grid P_5 when needed. These figures clearly illustrate how the proposed strategy reallocates energy among the PV system, battery, and grid in real time under these three scenarios.

4.3.2. Comparison between MOC and MSC

Fig. 14 shows the results of the MSC strategy. It can be observed that the power from the battery to the greenhouse (P_1) peaks at 7:00,

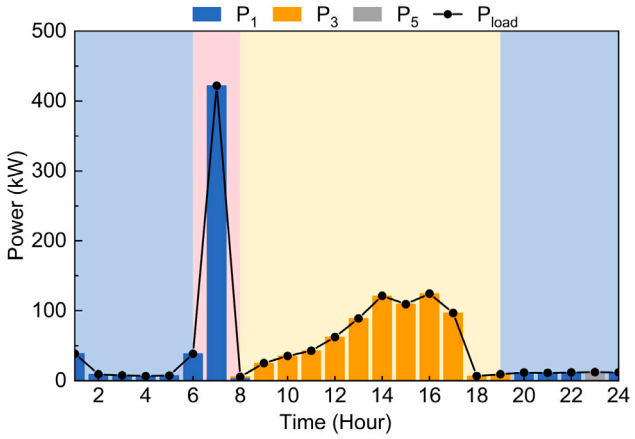

Fig. 13. Real-time energy allocation under different operating scenarios.

indicating the system is utilizing stored energy during the early morning. Between 10:00 and 16:00, the PV system provides power directly to the greenhouse (P_3) and charges the battery (P_2), with excess energy being exported to the grid (P_4). It indicates that the MSC strategy effectively maximizes self-consumption of solar energy during daylight hours, reducing reliance on the grid. By charging the battery during periods of excess PV generation, the system ensures sufficient energy is available for nighttime use, enhancing overall energy efficiency and reducing operational costs.

Fig. 15 illustrates a comparison between the proposed MOC and MSC strategies. The MOC strategy achieves a slightly lower clean energy SCR of 59.78% compared to the MSC strategy's 77.80%. Consequently, the MOC strategy results in a marginal increase in carbon emissions, with 13.00 kg of emissions and a carbon emission cost of R11.70, while the MSC strategy achieves zero carbon emissions and incurs no related costs. However, the MOC strategy demonstrates a clear advantage in terms of overall cost efficiency. Its energy cost is −R446.69, indicating that revenues from electricity sales exceed purchase costs, whereas the MSC strategy shows a lower energy cost savings of −R259.42. The battery aging cost under the MOC strategy is lower at R2754.10, while the MSC strategy incurs a higher battery aging cost of R3249.30. Despite the MOC strategy's slightly higher carbon emissions and lower SCR, it provides a more economical solution by effectively reducing overall costs. This balance of cost reduction while still maintaining a reasonable level of clean energy self-consumption highlights the practicality of the MOC strategy for cost-conscious operations.

4.4. Control of the hybrid energy system

To address the solar power generation fluctuations and load demand variations, an MPC approach is proposed to manage the hybrid energy system, ensuring a balanced power supply and demand. The optimal operation of the hybrid energy system produces the SOC, which serves as the reference trajectory that MPC is designed to follow. Furthermore, the optimized values of P_1, P_2, P_3, P_4, P_5, and P_6 are used as reference trajectories for the control inputs.

4.4.1. Control parameters setting

For MPC, the prediction horizon N_p and control horizon N_c are both set to 10. The weighting matrix $Q = \mathrm{Diag}(50)$, and the weighting matrix $R = \mathrm{Diag}(50, 50, 50, 50, 50, 50)$. This approach ensures precise control, maintaining system stability while efficiently balancing supply and demand. The load demand and PV generation disturbances can be introduced using random fluctuations, for example, a 10% load demand disturbance can be simulated with the formula: $P_{load} = P_{load} \times (1 + 0.1 \times$

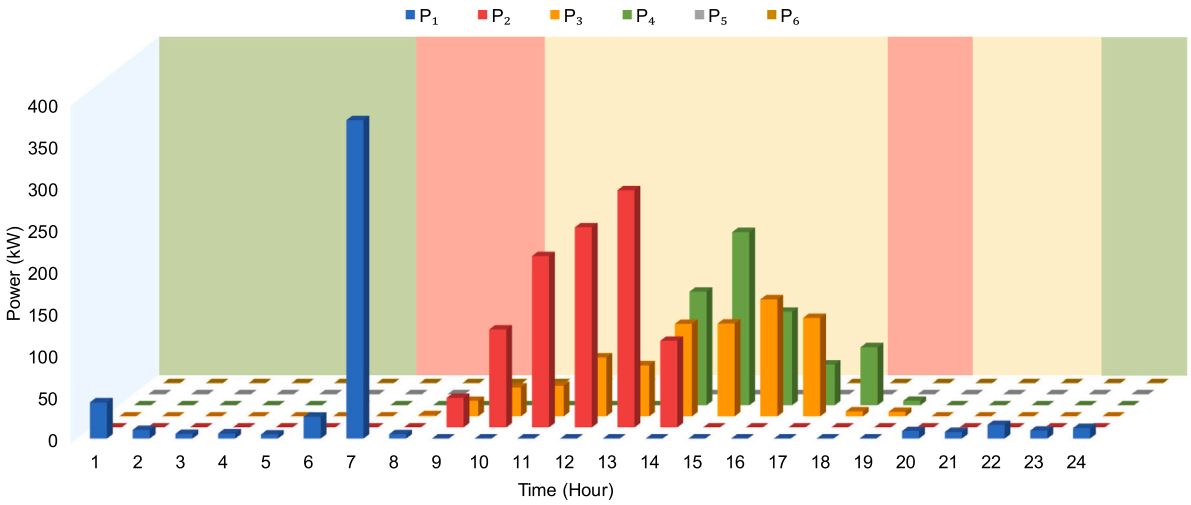

Fig. 14. Results of MSC strategy.

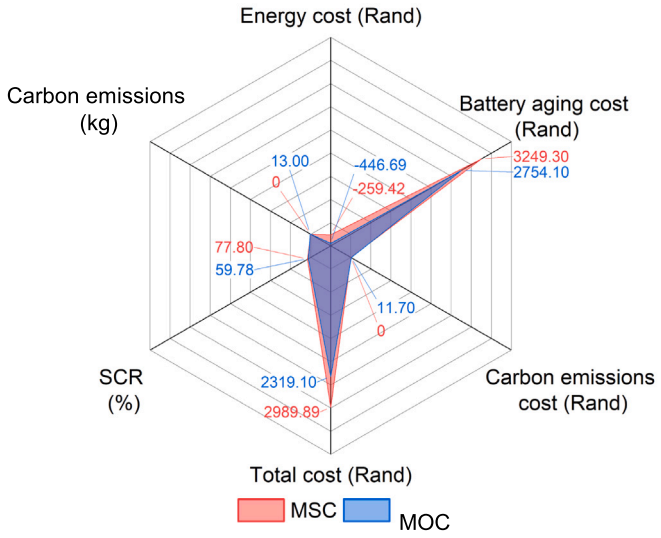

Fig. 15. Comparison between MOC and MSC strategy.

$(2\times rand(1,24)-1)$. Similarly, 20% and 30% disturbances can be applied using the same method by adjusting the disturbance factor to 0.2 or 0.3, respectively.

4.4.2. Comparison between MPC and open loop control

Fig. 16 compares the performance of MPC and commonly used open loop control under 10%, 20%, and 30% disturbances. The reference trajectory represents the load demand, with green representing power provided under the MPC and red representing power provided under the open loop control. Across all disturbance levels, MPC more closely follows the reference trajectory. As the disturbance increases, the deviation in open loop control grows more significant, particularly with a larger overshoot at the 30% disturbance level. In contrast, the MPC maintains better tracking accuracy, demonstrating its robustness and superior control in handling load disturbances compared to the open loop control.

4.5. Discussion

This study proposed an integrated optimization and control framework for managing greenhouse operations and hybrid energy systems dispatch. The results demonstrate that the MTC strategy, which simultaneously accounts for energy consumption, CO_2 supply, and CO_2 emissions, significantly outperforms strategies that focus solely on minimizing energy consumption or cost. By considering these interrelated factors, the proposed strategy effectively reduced both operational costs and carbon emissions while maintaining optimal conditions for plant growth.

For hybrid energy system scheduling, the MOC strategy, which incorporates battery aging costs alongside electricity purchase and sales, proved to be more cost-effective than the MSC strategy, which focuses primarily on energy consumption. The MOC strategy efficiently utilized renewable energy sources and extended battery life, demonstrating the importance of considering long-term cost factors. While the MSC strategy reduces reliance on the grid and lowers carbon emissions, it does not offer the comprehensive economic benefits of the proposed MOC strategy.

The MPC strategy showed robustness under various disturbance scenarios, maintaining system stability and offering better performance compared to an open loop control strategy. This underscores the robustness of the MPC in addressing uncertainties and strengthens its potential for greenhouse energy system optimization when coupled with renewable energy sources and carbon emissions management.

5. Conclusion

This study proposes a hierarchical model predictive control (MPC) framework for grid-connected PV battery systems in greenhouse environments, taking into account the energy-water-carbon-food (EWCF) nexus. The framework comprises three coordinated layers: a greenhouse operation optimization layer, a hybrid energy system management layer, and a real-time control layer. The key findings are summarized as follows:

(1) The MCE strategy, which considered time-of-use tariffs and shifted greenhouse load demand from high-price to low-price periods, increased energy consumption by 19.58% (1542.50 kWh vs. 1290.27 kWh) but reduced energy costs by 10.48% (R1986.44 vs. R2218.57) compared to the MEC strategy. These results demonstrate that cost-oriented energy scheduling can yield economic benefits, even with higher consumption levels.

(2) The MTC strategy, which simultaneously considers energy consumption, CO_2 supply and carbon emissions, achieved the lowest total cost and the best overall economic performance among the three greenhouse optimization strategies. The total cost under the MTC strategy (R4320.82) was reduced by 81.01% and 81.31%

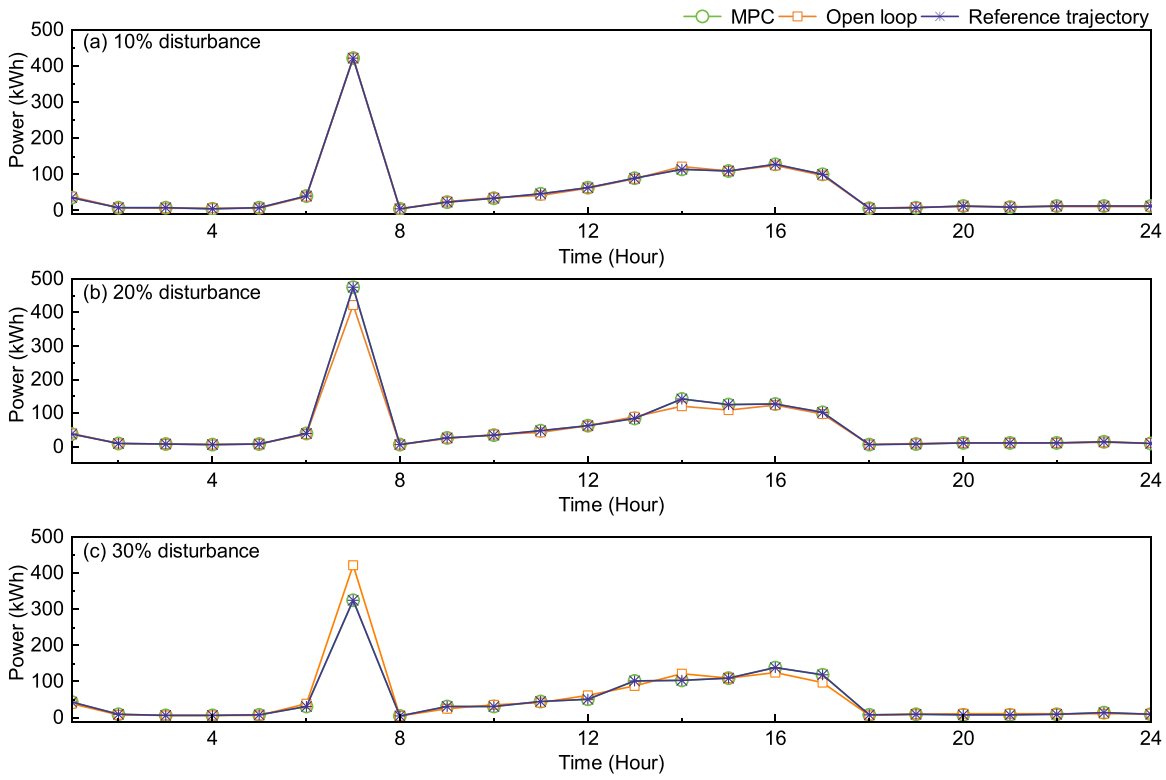

Fig. 16. Comparison of MPC and open loop control under different load disturbances.

compared with the MEC (R22743.70) and MCE (R23105.46) strategies, respectively. These results indicate that the MTC strategy provides a much more cost-effective approach to greenhouse operation than conventional MEC and MCE strategies.

(3) The MOC strategy, which incorporates battery aging and electricity purchase and sale costs, proved to be more cost-effective than the MSC strategy (R2319.10 vs. R2989.89). By optimizing renewable energy use and extending battery life, the MOC strategy balances immediate energy demands with long-term economic efficiency. In contrast, while the MSC strategy reduces grid reliance and carbon emissions, it does not provide equivalent economic benefits, highlighting the trade-off between immediate cost savings and the overall optimization of energy use and costs.

(4) MPC effectively tracked the reference trajectory, while open loop control exhibited significant deviations that increased with disturbance intensity. This highlights the robustness of MPC in handling uncertainties and underscores its potential to optimize greenhouse energy systems, making it a reliable choice for enhancing both performance and sustainability.

Future work will focus on the following directions: first, developing data-driven models for greenhouse systems to improve the accuracy and adaptability of optimization and control strategies; second, integrating additional renewable energy sources such as wind and biomass to enhance the sustainability and resilience of the energy system; and finally, conducting comprehensive uncertainty analyses to improve the robustness of the proposed framework and ensure reliable performance under real-world operating conditions.

CRediT authorship contribution statement

Dong Lin: Writing – original draft, Software, Methodology. **Minjie Hu:** Software, Formal analysis. **Zhiling Ren:** Resources, Investigation. **Yun Dong:** Supervision, Resources, Data curation. **Xianming Ye:** Supervision, Methodology. **Yuling Fan:** Validation, Formal analysis. **Lijun Zhang:** Supervision, Methodology, Conceptualization.

Declaration of Generative AI and AI-assisted technologies in the writing process

During the preparation of this work, the authors used ChatGPT to enhance language and readability. After using this tool, the authors reviewed and edited the content as needed and took full responsibility for the content of the publication.

Declaration of competing interest

The authors declare that they have no known competing financial interests or personal relationships that could have appeared to influence the work reported in this paper.

Acknowledgments

We acknowledge the financial support from the National Natural Science Foundation of China (Grant No. 61903149) and the Liaoning Province Education Department, China (Grant Nos. LJKZ0332, JYTQN2023197).

Data availability

Data will be made available on request.

References

[1] Achour Y, Ouammi A, Zejli D. Technological progresses in modern sustainable greenhouses cultivation as the path towards precision agriculture. Renew Sustain Energy Rev 2021;147:111251.

[2] Ajagekar A, Mattson NS, You F. Energy-efficient AI-based control of semi-closed greenhouses leveraging robust optimization in deep reinforcement learning. Adv Appl Energy 2023;9:100119.

[3] Guo Y, Zhao H, Zhang S, Wang Y, Chow D. Modeling and optimization of environment in agricultural greenhouses for improving cleaner and sustainable crop production. J Clean Prod 2021;285:124843.

[4] Chen W-H, Mattson NS, You F. Intelligent control and energy optimization in controlled environment agriculture via nonlinear model predictive control of semi-closed greenhouse. Appl Energy 2022;320:119334.
[5] Zhao Y, Li Z, Deger C, Wang M, Peric M, Yin Y, Meng D, Yang W, Wang X, Xing Q, et al. Achieving sustainability of greenhouses by integrating stable semi-transparent organic photovoltaics. Nat Sustain 2023;6(5):539–48.
[6] Munoz-Liesa J, Royapoor M, Cuerva E, Gassó-Domingo S, Gabarrell X, Josa A. Building-integrated greenhouses raise energy co-benefits through active ventilation systems. Build Environ 2022;208:108585.
[7] Iddio E, Wang L, Thomas Y, McMorrow G, Denzer A. Energy efficient operation and modeling for greenhouses: A literature review. Renew Sustain Energy Rev 2020;117:109480.
[8] Lin D, Dong Y, Ren Z, Zhang L, Fan Y. Hierarchical optimization for the energy management of a greenhouse integrated with grid-tied photovoltaic–battery systems. Appl Energy 2024;374:124006.
[9] Ge Q, Ke Z, Liu Y, Chai F, Yang W, Zhang Z, Wang Y. Low-carbon strategy of demand-based regulating heating and lighting for the heterogeneous environment in beijing venlo-type greenhouse. Energy 2023;267:126513.
[10] Hu G, You F. An ai framework integrating physics-informed neural network with predictive control for energy-efficient food production in the built environment. Appl Energy 2023;348:121450.
[11] Zou H, Wang F, Zeng Z, Zhu J, Zha L, Huang D, Li J, Wang R. Next-generation water-saving strategies for greenhouses using a nexus approach with modern technologies. Nat Commun 2025;16(1):2091.
[12] Hegazy A, Farid M, Subiantoro A, Norris S. Sustainable cooling strategies to minimize water consumption in a greenhouse in a hot arid region. Agricult Water Manag 2022;274:107960.
[13] Abedrabboh O, Koç M, Biçer Y. Modelling and analysis of a renewable energy-driven climate-controlled sustainable greenhouse for hot and arid climates. Energy Convers Manage 2022;273:116412.
[14] Ahmadbeyki A, Ghahderijani M, Borghaee A, Bakhoda H. Energy use and environmental impacts analysis of greenhouse crops production using life cycle assessment approach: A case study of cucumber and tomato from tehran province, Iran. Energy Rep 2023;9:988–99.
[15] Twala S, Ye X, Xia X, Zhang L. Optimal integration of solar home systems and appliance scheduling for residential homes under severe national load shedding. J Autom Intell 2023;2(4):227–38.
[16] Murei A, Kamika I, Momba MNB. Selection of a diagnostic tool for microbial water quality monitoring and management of faecal contamination of water sources in rural communities. Sci Total Environ 2024;906:167484.
[17] Our world in data, global fossil fuels share of energy. 2023, https://ourworldindata.org/grapher/fossil-fuels-share-energy. [Accessed 24 September 2024].
[18] Liu T, Yuan Q, Wang Y. Hierarchical optimization control based on crop growth model for greenhouse light environment. Comput Electron Agric 2021;180:105854.
[19] Katzin D, Marcelis LF, van Mourik S. Energy savings in greenhouses by transition from high-pressure sodium to led lighting. Appl Energy 2021;281:116019.
[20] Luqman M, Mahmood F, Al-Ansari T. Supporting sustainable global food security through a novel decentralised offshore floating greenhouse. Energy Convers Manage 2023;277:116577.
[21] Ouammi A, Achour Y, Zejli D, Dagdougui H. Supervisory model predictive control for optimal energy management of networked smart greenhouses integrated microgrid. IEEE Trans Autom Sci Eng 2019;17(1):117–28.
[22] Ravishankar E, Booth RE, Saravitz C, Sederoff H, Ade HW, O'Connor BT. Achieving net zero energy greenhouses by integrating semitransparent organic solar cells. Joule 2020;4(2):490–506.
[23] Chen W-H, You F. Decarbonization through smart energy management: Climate control in building-integrated rooftop greenhouses for urban agriculture across various climate conditions. J Clean Prod 2024;458:142544.
[24] Ali RB, Bouadila S, Arıcı M, Mami A. Feasibility study of wind turbine system integrated with insulated greenhouse: Case study in tunisia. Sustain Energy Technol Assess 2021;47:101333.
[25] Mahmood F, Al-Ansari T. Design and analysis of a renewable energy driven greenhouse integrated with a solar still for arid climates. Energy Convers Manage 2022;258:115512.
[26] Jin Y, Jiang W, Han Y, Nan S, Liu G, Guo W, Zhang K, Li Q, Li D. Comprehensive optimization of shading and electrical performance of roof-mounted photovoltaic system of venlo-type greenhouse in the severe cold region. Energy 2024;296:131125.
[27] Gorjian S, Ebadi H, Najafi G, Chandel SS, Yildizhan H. Recent advances in net-zero energy greenhouses and adapted thermal energy storage systems. Sustain Energy Technol Assess 2021;43:100940.
[28] Manesh MHK, Davadgaran S, Rabeti SAM. Novel solar-biomass polygeneration system based on integration of ICE-ORC-MDC-HDH-RO and tomato greenhouse to produce power, freshwater, and biological wastewater treatment. Energy Convers Manage 2024;308:118349.
[29] Nasrabadi AM, Malaie O, Moghimi M, Sadeghi S, Hosseinalipour SM. Deep learning optimization of a combined cchp and greenhouse for co2 capturing; case study of tehran. Energy Convers Manage 2022;267:115946.
[30] Fu X, Bai J, Sun H, Zhang Y. Optimizing agro energy environment synergy in agricultural microgrids through carbon accounting. IEEE Trans Smart Grid 2024.
[31] Ouammi A. Model predictive control for optimal energy management of connected cluster of microgrids with net zero energy multi-greenhouses. Energy 2021;121274.
[32] Lin D, Zhang L, Xia X. Model predictive control of a Venlo-type greenhouse system considering electrical energy, water and carbon dioxide consumption. Appl Energy 2021;298:117163.
[33] Mahmood F, Govindan R, Bermak A, Yang D, Al-Ansari T. Data-driven robust model predictive control for greenhouse temperature control and energy utilisation assessment. Appl Energy 2023;343:121190.
[34] Jiao F, Zou Y, Zhang X, Zhang B. Online optimal dispatch based on combined robust and stochastic model predictive control for a microgrid including EV charging station. Energy 2022;247:123220.
[35] Van Beveren P, Bontsema J, Van Straten G, Van Henten E. Minimal heating and cooling in a modern rose greenhouse. Appl Energy 2015;137:97–109.
[36] Van Beveren P, Bontsema J, Van Straten G, Van Henten E. Optimal control of greenhouse climate using minimal energy and grower defined bounds. Appl Energy 2015;159:509–19.
[37] Hussain A, Choi I-S, Im YH, Kim H-M. Optimal operation of greenhouses in microgrids perspective. IEEE Trans Smart Grid 2018;10(3):3474–85.
[38] van Beveren P, Bontsema J, van't Ooster A, van Straten G, van Henten EJ. Optimal utilization of energy equipment in a semi-closed greenhouse. Comput Electron Agric 2020;179:105800.
[39] Kuijpers WJ, Katzin D, van Mourik S, Antunes DJ, Hemming S, van de Molengraft MJ. Lighting systems and strategies compared in an optimally controlled greenhouse. Biosyst Eng 2021;202:195–216.
[40] Parada F, Gabarrell X, Rufí-Salís M, Arcas-Pilz V, Muñoz P, Villalba G. Optimizing irrigation in urban agriculture for tomato crops in rooftop greenhouses. Sci Total Environ 2021;794:148689.
[41] Campana PE, Li H, Zhang J, Zhang R, Liu J, Yan J. Economic optimization of photovoltaic water pumping systems for irrigation. Energy Convers Manage 2015;95:32–41.
[42] Yan H, Deng S, Zhang C, Wang G, Zhao S, Li M, Liang S, Jiang J, Zhou Y. Determination of energy partition of a cucumber grown Venlo-type greenhouse in southeast China. Agricult Water Manag 2023;276:108047.
[43] Adefarati T, Bansal R, Shongwe T, Naidoo R, Bettayeb M, Onaolapo A. Optimal energy management, technical, economic, social, political and environmental benefit analysis of a grid-connected PV/WT/FC hybrid energy system. Energy Convers Manage 2023;292:117390.
[44] Wu Y, Liu Z, Liu J, Xiao H, Liu R, Zhang L. Optimal battery capacity of grid-connected PV-battery systems considering battery degradation. Renew Energy 2022;181:10–23.
[45] Ren Z, Dong Y, Lin D, Zhang L, Fan Y, Xia X. Managing energy-water-carbon-food nexus for cleaner agricultural greenhouse production: A control system approach. Sci Total Environ 2022;848:157756.
[46] Weidner T, Yang A, Hamm MW. Energy optimisation of plant factories and greenhouses for different climatic conditions. Energy Convers Manage 2021;243:114336.
[47] Zou B, Peng J, Li S, Li Y, Yan J, Yang H. Comparative study of the dynamic programming-based and rule-based operation strategies for grid-connected PV-battery systems of office buildings. Appl Energy 2022;305:117875.
[48] Zhang Y, Ma T, Yang H. Grid-connected photovoltaic battery systems: A comprehensive review and perspectives. Appl Energy 2022;328:120182.
[49] Hu G, You F. Multi-zone building control with thermal comfort constraints under disjunctive uncertainty using data-driven robust model predictive control. Adv Appl Energy 2023;9:100124.
[50] Zou B, Peng J, Yin R, Luo Z, Song J, Ma T, Li S, Yang H. Energy management of the grid-connected residential photovoltaic-battery system using model predictive control coupled with dynamic programming. Energy Build 2023;279:112712.